Comparative Morphological Characterization of Skin after Subcutaneous Application of Hyaluronic Acid and Polycaprolactone in Rats: Establishment of an Experimental Model

Cintia Melo Braga
Federal University of Ceará
Conceicao da Silva Martins Rebouças
Federal University of Ceará
Deborah Nunes Melo
Federal University of Ceará
Ana Paula Negreiros Nunes
Federal University of Ceará
Paula Góes
Federal University of Ceará
Maria Luana Gaudencio dos Santos Morais
Federal University of Ceará
Gerly Anne Castro Brito
Federal University of Ceará
Renata F.C Leitão (renata.carvalho@ufc.br)
Federal University of Ceará

Research Article

Keywords: dermal fillers, polycaprolactone, hyaluronic acid

Posted Date: June 28th, 2023

DOI: https://doi.org/10.21203/rs.3.rs-3097593/v1

Additional Declarations: No competing interests reported.

Abstract

Injectable facial fillers are excellent options for treating facial aging, wrinkles, and contour defects. Both polycaprolactone (PCL) and hyaluronic acid (HA) have been used to restore lost tissue volume and improve facial contour. However, the mechanisms involved in the effect of these biomaterials still need to be fully understood. The present work aims to establish an experimental model to investigate cellular and morphological changes in the skin of Wistar rats in response to HA and PCL to understand the mechanisms associated with these effects. The subcutaneous tissue of the back of Wistar rats was used as a reception area for biomaterials, represented by the commercial products Ellansé®, containing polycaprolactone (PCL) and Juvederm Voluma®, containing hyaluronic acid (HA). Animals were euthanized afetr 30 or 60 days, and skin samples were collected from treated and untreated animals (CONTROL) for histological and immunohistochemical evaluation for IBA-1, TGF-β, and FGF. Analysis of type I and type III collagen deposition, neovascularization, and adipose tissue was performed. On histological examination, HA appeared as an amorphous, basophilic material interspersed with connective tissue bundles. The skin fragments with PCL showed intense cell proliferation, with foreign body giant cells and a higher capillary proliferation than the HA group. More vessels were observed in the HA and PCL groups compared to the CONTROL group. A significant increase in fibroblasts and fibrocytes was observed in skin fragments inoculated with HA and PCL, associated with increased FGF expression. The number of fibroblasts was significantly higher in the PCL group than HA. The PCL group showed higher immunostaining for IBA-1 and TGF-β than the CONTROL and HA groups. Collagen deposition was observed in the treated groups, especially type III collagen in the PCL group, when compared to HA. Our morphological results demonstrated stimulation of fibroblastic activity and active-related tissue regeneration, with increased vascular proliferation and expression of markers related to tissue proliferation, mainly associated with the PCL group. We also observed increased adipose tissue, although further studies are needed to confirm these findings.

1 INTRODUCTION

Like other organs, the skin undergoes a natural aging process over time. Moreover, it is directly exposed to environmental damage, especially ultraviolet radiation (UV)[1]. Because of this process, contour deficiencies, wrinkles, loss of dermal matrix, and decreases in collagen and elastic fibers appear, resulting in a reduction of elasticity [2–4]. In addition to skin aging, three-dimensional losses are seen in the face, involving bones, muscles, and fat pads that affect the aged appearance. Many dermal fillers have been used to minimize these losses, filling in wrinkles and restoring the volume of tissue lost, either due to disease or aging [5]. Soft tissue fillers are less invasive with less downtime than traditional surgical interventions[6]. One of the most used dermal fillers is hyaluronic acid (HA) due to its biocompatibility, non-immunogenicity, biodegradability, and high-water absorption capacity. HA performs different functions, such as lubrication, hydration, and maintenance of tissue structure. In addition, it is involved in cell proliferation and migration events, as well as angiogenesis [7].

Another material used for filling purposes is polycaprolactone (PCL), a polymer that provides safe and lasting correction of aging-related volume loss or changes in facial contour. The main aesthetic results obtained with PCL are volume restoration, contour redefinitions, and wrinkle reduction. Its positive effect on skin quality has also been widely reported. The safety profile, easy injection, and adjustable longevity are determining factors in choosing this product [7, 8]

Substances that restore lost tissue volumes, such as HA and PCL, are highlighted in this context. However, the mechanisms involved in the effect of these materials still need to be fully understood. Therefore, the present work aims to establish an experimental model to investigate the morphological changes in the skin after PCL and HA injections through histomorphometry and autofluorescence techniques.

2 METHODS

2.1 Study design and ethical aspects

The present study was randomized, controlled, and blinded. The Guidelines conducted surgical procedures and animal treatments for Institutional and Animal Care and Use (CEUA) of the Federal University of Ceará, Brazil (#7904140420 / 2020).

2.2 Animals

Sixteen heterogeneous male Wistar rats, 200-250g, from the UFC central vivarium, were maintained in an environment-controlled room with a 12-h light/12-h dark cycle. The animals were kept in standard plastic cages with metal lids, with four animals per cage, and received water and food *ad libitum*. Every effort was made to reduce the number of animals used and their pain, suffering, and stress.

Preparation of animals

2.3 Dermal Fillers

In the present study, Juvéderm Voluma® (Allergan®) and Ellansé® (Sinclair Pharma, London, UK) fillers were used. Juvéderm Voluma® is a homogenized dermal filler composed of cross-linked hyaluronic acid at 20 mg/ml concentration in a physiological buffer with lidocaine. Juvéderm Voluma® is derived from Streptococcus equi and cross-linked with diglycidyl ether 1,4-butanediol (BDDE) in a one-step cross-linking process in which high and low molecular weight molecules are mixed. Ellansé® is a PCL-based collagen stimulator with 30% synthetic PCL microspheres suspended in 70% aqueous carboxymethyl cellulose.

2.4. Experimental model for the injection of dermal fillers

The animals were anesthetized with ketamine (80 mg/kg, i.p.) and xylazine (10 mg/kg, i.p.), and, in the following, the animals' backs were trichotomized. Samples were injected in boluses of 0.05 ml, containing PCL or HA, in the subcutaneous tissue of the animals' backs, just below the panniculus

carnosus, using a 26G needle. Each animal received both biomaterials injected in two different points of the dorsal-lateral region, respecting a minimum distance of 5cm between them. They were followed up daily for seven days to verify signs of acute inflammation at the inoculation sites. The animals were euthanized with an overdose of 2% xylazine (30mg/kg) and 10% ketamine (240mg/kg) thirty (n = 8) or sixty (n = 8) days after the injection of the fillers. The skin on the back of each animal was folded back, allowing visual inspection of the subcutaneous tissue with the fillers. Signs of inflammation and fibrosis were investigated, and the volume gain related to each filler was observed. Next, skin samples containing HA, PCL, as well as skin samples with no fillers (CONTROL) were surgically removed and divided into two fragments: one fixed in 10% buffered formalin and the other stored at -80°C for further processing for histological slides and protein extraction, respectively.

2.5 Histopathological analysis

The tissues fixed in 10% buffered formalin were processed for paraffin embedding. Histological slides were prepared using 4µm thick tissue sections, stained with hematoxylin and eosin (HE), Mallory's trichrome, and picrosirius red. An experienced pathologist, who did not know which were the control or treatment samples, performed all histological analyses. HE stained sections were qualitatively evaluated in at least 6 (six) specimens *per* group, considering five fields per slide, at a magnification of 200x. Inflammatory findings such as cellular infiltrate, edema, and hemorrhage were investigated. We also counted fibroblasts and fibrocytes in at least six slides of each group, HA, PCL, and CONTROL, considering five fields per slide at 400x magnification. As for the slides stained with Mallory's Trichrome, the effect of biomaterials on the connective tissue vasculature at the periphery of the implants was investigated by quantifying the number of blood vessels and the total vessel area. At least six specimens per group were used. Initially, the areas of greatest vascularization were identified (hot spots) for delimitation and measurement of the areas of the ten largest blood vessels, considering the cross-sectional diameter, from digitalized images. The images were captured using a digital camera attached to a Leica microscope at 400x magnification and analyzed with LAS V3.7.0 software [9]

The quantification of the vessels was also performed by observing five fields per slide and six specimens per group, at 200X magnification. The slides stained with picrosirius red were photographed with a DFC 295 camera attached to the optical microscope under polarized light (Leica DM 2000). Evaluation of type I and III collagen fiber deposition was performed at the periphery of the biomaterials after light polarization, allowing differentiation of type I (yellowish orange to orange and red birefringence) and type III (green or yellow-green birefringence) collagen. From each slide, 10 histological fields were selected and photomicrographed at 400x magnification. The images were analyzed using the computational program Photoshop to obtain the collagen percentage by automated particle analysis according to the selection and measurement of the areas based on color. The values for each collagen type in Threshold Color were standardized for all images.

2.6 Immunohistochemical analysis

Immunohistochemical analyses for IBA-1, TGF-β and FGF were performed in CONTROL, PCL, and HA groups by the streptavidin-biotin peroxidase method in formalin [10]. Tissue sections were fixed in paraffin-embedded, cut four μm thick, and prepared in poly-L-lysine-coated microscope slides. After deparaffinization, antigenic recovery was performed with citrate buffer recovery solution (pH 6.0) for 20 minutes at 95°C. The endogenous peroxidase was blocked with 3% H2O2 for 10 minutes to reduce non-specific binding. The sections were then incubated with anti-IBA-1 (dilution 1: 100; Santacruz Biotechnology; California, USA), anti-TGFβ (dilution 1: 100; Santacruz Biotechnology; California, USA), anti-FGF (dilution 1: 100; Santacruz Biotechnology; California, USA) diluted in DAKO antibody diluent for 1 h. The antibody binding sites were visualized by incubation with diaminobenzidine-H2O2 solution (DAB, DAKO; California, USA). In parallel, negative control without the primary antibody was performed. The slides were counterstained with hematoxylin, dehydrated in graded alcohol series, clarified in xylene, and covered with a coverslip. Positivity for IBA-1, TGF-β, and FGF was determined by brown staining at the cytoplasmic level in the connective tissue. Cytoplasmic quantification of immunolabeled cells was performed on at least 6 slides per group. From each slide, 5 histological fields (400x magnification) were selected and photomicrographed with a digital camera attached to an optical microscope (Leica DM 2000, Wetzlar, Germany). The images were analyzed using the computational program Photoshop 8.0 to quantify the percentage of immunolabeled area. The percentage of the immunolabeled area was calculated from the ratio between the immunolabeled area (in pixels) multiplied by 100 and the total area (in pixels), as previously described [11]

2.7 Western blot analyses

First, 20μg of protein of each sample was prepared from frozen tissue by adding sample buffer (BioRad, USA 65.8 mM Tris-HCl, pH 6.8; 26.3% glycerol; 2.1% SDS; 0.01% bromophenol blue) and βmercaptoethanoll (BioRad, USA) and vortexing for 10 seconds. Plus, heating in a water bath (95°C, 5 min) and spinning (10000 rpm, 4°C, 30s). Next, vertical polyacrylamide-SDS gel electrophoresis of proteins (SDS-PAGE) was performed at 60 v for the first 15 min for deposition of samples at the bottom of the well; and 120 v for the rest of the run, where 10% gel (FGF, and β-actin) and race buffer (25 mM Tris; 192 mM glycine; 1% SDS) were used. After the run, transfer of the proteins from the gel to the PVDF membrane (BioRad, USA, Polyvinylidene Fluoride) was performed at 100-fold for two hours in transfer buffer (25 mM Tris; 192 mM glycine; 20% methanol). After this step, the membranes were blocked for one hour under constant agitation, to reduce nonspecific binding, with 5% BSA (Sigma-Aldrich, USA) diluted in Tris-HCl saline buffer supplemented with Tween 20 (TBST- 20 mM Tris pH 7.5; 150 mM NaCl; 0.1% Tween 20). Next, the membranes were washed with TBST, with three washes for 10 min each. In the next step, the membranes were incubated overnight at 4°C under constant agitation, with the FGF (1:100; Invitrogen, USA) or anti-β-actin (1:200; Santa Cruz, USA) antibodies diluted in 1% BSA in TBST. After this step, three washes of 10 min each with TBST were performed. The membranes were incubated with the HRP-goat anti-rabbit secondary antibodies (1:1000; Invitrogen, USA) for two hours at room temperature. After this time, the membranes were washed thrice with 10 min duration each, using TBST. Chemiluminescence reagent (BioRad, USA, Clarity western ECL blotting substrate) was added, and the membranes were shaken for 5 min. Images of the bands were captured by a ChemiDoc XRS system (BioRad, USA) or

exposed to radiographic film. The density of the bands was measured using ImageJ software (NIH, Bethesda, MD, USA).

2.8 Statistical analysis

Data are presented as mean ± SEM. Analysis of variance (ANOVA) was followed by Tukey's test, using GraphPrism (GraphPad 6.0 Software Inc., La Jolla, CA, USA). The significance level adopted was ($p < 0.05\%$) for all analyses.

3 RESULTS

3.1 Visual inspection of changes induced by HA and PCL in the skin of *Wistar* rats.

When the animal's posterior skin was folded (Fig. 1A), it was possible to macroscopically observe an increase in tissue volume at the points where the fillers were applied, suggesting the presence of PCL (Fig. 1B) and HA (Fig. 1C) in the subcutaneous tissue. The HA recipient point was nodular and translucent, with an elastic consistency and a smooth surface. The surface was homogeneous and elastic when the tissue was cut into two fragments. The spot that received PCL inoculation had irregular, slightly raised, whitish edges with a firm consistency and a granular surface when cut.

3.2 Microscopic changes induced by HA and PCL in the skin of *Wistar* rats.

The biological response to the administration of the biomaterials was examined histologically to investigate the effects of HA and PCL. Figure 1D shows the stratification of the rodent skin with the application of the biomaterials below the panniculus carnosus. Thirty days after the subcutaneous administration, the HA group presented as an amorphous, slightly basophilic material, dissociating fat lobes (Fig. 1F, 1I). The biomaterial (HA) was also intercalated with connective tissue bundles. No histologically apparent tissue reaction was observed, except for small, sporadic nuclear aggregates compatible with foreign giant body cells and the presence of adipose tissue at the periphery of the material, as illustrated in Fig. 1O. In some areas, a discrete capillary proliferation was also observed, always associated with the presence of the injected substance.

In the PCL samples, the marked cellular proliferation of cells with granular cytoplasm, nuclei mostly eccentric, small, round, and with fine chromatin compatible with macrophages, was observed. The increase of small vessels was observed, as well as loose connective tissue, with focal areas showing thicker collagen bundles, demonstrating moderate fibrosis (Figs. 1G, 1J). This connective tissue was found between the material particles at the periphery of the PCL mass. After sixty days, small capillaries persisted in HA, but with a more regular distribution, without denoting considerable tissue reaction (Fig. 1L). In the samples with PCL, there was less cellularity, fewer granular cells, more fibrous connective

tissue between the material particles, and more closely spaced cells with bundles of collagen fibers (Fig. 1M). The presence of capillaries was maintained when compared to 30 days.

3.3 Effect of biomaterials on cell proliferation and neovascularization

The presence of nuclear aggregates and fusion of epithelioid cells, which is compatible with activated macrophages, were observed by immunoglobulin analysis for IBA-1 (Fig. 2A), characterized by marking cells with brownish staining in the skin of mice subjected to HA and PCL injection. After 30 days of biomaterial administration, this analysis showed a significant increase in activated macrophages in HA and PCL compared to the CONTROL group and a higher presence of activated macrophages in PCL compared to HA ($p < 0.05$). After 60 days, the pattern of macrophage activity showed a slight reduction in the treated groups, in which only the HA group had a significant decrease in its activity compared to the 30 and 60-day periods.

Immunohistochemical analysis showed, after 30 days, a significant increase in TGF-β immunohistochemistry in the HA and PCL groups compared to the CONTROL group. Still, there was no statistical difference between them. After 60 days, there was a significant decrease in immunolabeling in the HA and PCL groups compared to the previous period (30 days). A statistical difference was observed between the two treated groups, in which the PCL group had higher labeling than the HA group in the same period, as illustrated in the graph in Fig. 2B.

The vascular proliferation observed on the HE-stained slides was quantified using Mallory's Trichrome staining (Fig. 2C), which allowed the measurement of vessel area and number. As for the number of vessels, after 30 days of the injection period, a statistically significant increase was observed in both the HE and PCL groups compared to the control group. In addition, the PCL group showed an even more substantial number of vessels than HA ($p < 0.05$). After 60 days, there was a reduction in the number of vessels in the experimental groups, HA and PCL. However, there was still a significant increase in vessels in these groups when compared to the CONTROL group, which can be seen in the graph in Fig. 2C. However, no effect of biomaterials on vessel area was observed in any of the periods studied, as seen in the graph and illustrated in the images (Fig. 2C).

The histopathological analysis also showed an increase in the number of fibroblasts and fibrocytes, especially in the first 30 days after the injection of the biomaterials. The increase was significant for both cell types in the HA and PCL groups compared to CONTROL ($p < 0.05$). A more significant number of these cells was observed in the PCL group compared to -HA ($p < 0.05$) in both periods, followed in Fig. 3B.

A. Immunostaining for FGF at 30 and 60 days and quantification of 1 expressed in the graph. **B.** Fibrocyte and fibroblast count at 30 and 60 days represented in the graph. **C.** Illustrative image of the fibrocyte and fibroblast in the connective tissue adjacent to the biomaterial. Bars show mean ± SEM of 6 animals per group. * represents the significant difference of HA and PCL when compared to CONTROL, at 30 and 60

days. # represents the significant difference between PCL and HA. (*p < 0.001), ANOVA followed by Tukey's test).

The immunohistochemical analysis for FGF showed that after 30 days, there was a significant increase in the immunoexpression of this cytokine in the PCL group when compared to CONTROL and HA, as can be seen in Fig. 3C and confirmed in the representative images of brownish staining in the cytoplasm of the fibroblasts. As for the 60 days, the immunostaining for FGF became higher in both treated groups compared to CONTROL. However, no statistical difference was observed between them, which can be seen in the graph of Fig. 3A, which shows the quantification of these cells and the protein expression of FGF.

Collagen deposition in the biomaterial-treated skin was evaluated after 30 and 60 days using histological sections stained with picrosirius red, observed under a polarized light microscope. No significant difference was observed in the deposition of type I collagen in the periods evaluated, nor between the groups. Organized reddish-yellow fibers represent this collagen in both HA and PCL groups ($p < 0.001$) (Fig. 4) In these groups, a dominance of type III collagen, represented by green fibers, was observed, as shown in the illustrations and confirmed in the graphs quantifying the areas marked in red and green, representing type I and III collagen, respectively.

4. DISCUSSION

Fillers are the most widely used substances in aesthetic medicine [12] and are a viable alternative to surgery for patients seeking a safe, minimally invasive, and affordable means of maintaining a youthful appearance and correcting facial contour deficiencies[13]. These products have become a staple in aesthetic and medical procedures. A wide variety of options are available on the market, but the mechanisms associated with their effects still need to be fully understood [14]

It is known that the physiological reactions induced by these biomaterials are conditioned by their physical and biochemical properties, patient characteristics, and the injection technique used [15]. To better understand the biological interaction played by fillers, rodent models have proven to be a helpful tool, assessing, in addition to morphological changes in the skin, the lifting capacity, and the resistance to tissue deformation [16].

Traditionally, these experimental models inoculate the biomaterials into the dermal layer [17–20], one of the injection planes used to apply fillers. However, for safety purposes, most practitioners in the clinic use blunt cannulas for the injections, making filling at the dermal level impractical. The injection plane becomes subcutaneous with a blunt cannula, a trend in use today [21]. For this reason, the experimental model standardized in the present study evaluates the effects of the subcutaneous application of fillers.

Rodent skin differs from human skin, which must be considered in experimental studies. In rodents, the epidermis is thin and has a high density of hair follicles. The dermal white adipose tissue is delicate and lies directly beneath the reticular dermis, clearly separated from the subcutaneous white adipose tissue

by a muscular layer called the panniculus carnosus [22]. Although many other mammals, including humans, do not have the panniculus carnosus, layers of adipose tissue exist beneath the reticular dermis in several species, including pigs and humans [23]

Considering the proposal of applying fillers at the subcutaneous level, we initiated the development and standardization of our experimental model, evaluating morphological changes in Wistar rats' skin after using hyaluronic acid (HA) and polycaprolactone (PCL). The increasing worldwide demand for soft tissue fillers motivated us to investigate the direct action of these materials on intimal tissue.

Visual inspection of the rat's skin after euthanasia and histopathological analysis in both periods evaluated confirmed the biocompatibility with no clinical, macro, or microscopic signs of inflammation. The folded skin showed that the HA had a nodular appearance, and its volume appeared to increase after 30 days of biomaterial inoculation. In tissues with PCL, there was volume loss after 30 and 60 days, visually observed right after the Ellansé application. With 70% CMC in its composition, Ellansé, presents a general decrease in volume due to the reabsorption of this vehicle after one month. Connective tissue and neoformed vessels replace approximately 50% of the original CMC volume. The key to maintaining volume after injection of PCL-based filler is the formation of new vessels and collagen deposition [24], as observed in the present study, suggesting the volumizing capacity of PCL is smaller than hyaluronic acid's capacity.

According to the literature, HA promotes volumization and has an essential hygroscopic function, contributing to volume gain[25]. Histological analysis confirmed the presence of the biomaterials in the subcutaneous tissue below the panniculus carnosus skeletal muscle layer. The HA group showed mild neovascularization and an apparent increase in adipose tissue in the peri-implant region. Some authors consider HA to be minimally immunogenic, making it the most commonly used temporary filler with clinically satisfactory results in terms of volume. In the present study, this fact is corroborated by the increase in the volume of the area that received HA, 30 and 60 days after application. Hyaluronic acid dermal fillers are now considered the preferred material for minimally invasive cosmetic interventions [26]. Because HA does not show specificity for any organ or species, HA is considered immunologically inert [27, 28]. According to papers published in the literature, once injected into the skin, HA causes a mild inflammatory reaction at the host tissue boundary followed by a gradual fibrous growth, which anchors the gel to the surrounding host tissue, preventing product migration [29]. Our macroscopic and histological analyses after 30 and 60 days did not detect any evidence of acute inflammation. We observed that HA induces a discrete formation of fibrous connective tissue, which probably contributes to preventing material displacement. In addition, we observed an increase in adipose tissue at the periphery of the HA; however, no measurements were taken, and further studies are needed to confirm this finding. In 2020, Nadra and colleagues demonstrated in *in vitro* studies that treatment with cross-linked HA showed beneficial effects on cell adhesion and survival and reduced basal and induced lipolysis in fully mature adipocytes.

In this work, cross-linked HA promoted cell adhesion and preserved the adipogenic capacity of pre-adipocytes during prolonged cell culture, bringing additional evidence of the beneficial role of cross-linked HA-based fillers in maintaining subcutaneous fat. On the other hand, another paper published in 2017 demonstrated that HA promoted the proliferation of adipose tissue-derived stem cells and the differentiation of these cells into adipocytes, suggesting an action of HA related to increasing the number of adipocytes [30]. The presence of adipose tissue associated with PCL, appeared less evident when compared to HA and more apparent when compared to CONTROL. However, further studies are needed to confirm this finding. We found no evidence in the literature to support this finding. When analyzing the PCL samples, we identified, among the particles of the material, intense cell proliferation, and neovascularization, besides deposition of extracellular matrix between the particles and discrete collagen deposition. Some foci of the CMC carrier were also observed at 30 and 60 days. After 60 days, the cellularity decreased, showing an apparent increase in collagen deposition between the particles when compared to the 30-day analysis. There are reports in the literature that the CMC itself, the carrier of the PCL particles, seems to stimulate the tissue reaction until the complete resorption of the biomaterial is found in some giant cells in its periphery [31]. It is well established in the literature that the presence of biomaterial can induce a foreign body reaction, where monocytes migrate into the tissue, becoming macrophages, which, together with platelets, synthesize platelet-derived growth factor (PDGF) and transforming growth factor beta (TGFβ), which promote the migration of fibroblasts [32]. It was observed, through immunohistochemistry for IBA-1, the appearance of a higher number of activated macrophages in the experimental HA and PCL groups when compared to the control group (CONTROL). This increase was more expressive in the 30-day evaluation, with a more significant number of activated macrophages in the samples with PCL compared to HA, and both (HA and PCL) showed greater immunolabeling for IBA-1 when compared to the CONTROL group. There was a significant reduction of activated macrophages in the HA group at 60 days, but the statistical difference concerning the CONTROL group was maintained. The number of activated macrophages in the PCL group remained high after 60 days, and there was no significant difference in IBA-1 immunolabeling between the 30 and 60-day analyses. The higher number of macrophages in this group is probably related to the physical characteristics of the polycaprolactone, which presents as immunologically inert microspheres large enough to induce macrophage aggregation.

As mentioned earlier, macrophages release TGF-β, regulating cell behavior. TGF-β is known to be a potent chemoattractant for endothelial cells and fibroblasts, as well as for cells of innate immunity, such as neutrophils and monocytes[33], TGF-β can be considered an essential physiological regulator both for the maintenance of the extracellular matrix and also in tissue repair processes [34]. In the present study, we observed significant differences in immunostaining for TGF-β between the HA and PCL groups compared to the CONTROL group in the 30 and 60-day analyses. A substantial increase in TGF-β expression was observed in the 60-day analyses in the PCL group compared to HA, which was not observed at 30 days. Immunolabeling was observed mainly in the cytoplasm of macrophages. The significant increase in TGF-β immunolabeling in the PCL group compared to HA after 60 days is related to the higher expression of IBA-1 observed in PCL since the expression of TGF-β by macrophages is well established in the literature.

Moreover, the significant increase of fibroblasts in HA and PCL groups, compared to CONTROL, also contributes to understanding the higher expression of TGF-β in these groups. Although macrophages are the primary source of TGF-β, studies demonstrate fibroblasts' expression of this growth factor, especially during repair processes [35], closing a cycle in which TGF-β expressed by macrophages is a potent chemoattractant for fibroblasts, which in turn can express TGF-β.

The present study observed a significant increase in fibroblasts and fibrocytes in the HA and PCL groups compared to CONTROL at the evaluated periods. Fibroblasts are the most abundant cells in the dermis. These cells' essential characteristics are their ability to synthesize and remodel ECM. In a repair process, fillers work as a framework for the proliferation of these cells, which are the primary basis for fibrogenesis [36]. The literature further describes the chemoattractant role of TGF-β for endothelial cells [37]. Our study observed a significant increase in small vessels and capillaries in the HA and PCL groups, 30 days after inoculations compared to CONTROL. In contrast to that observed in HA, The number of vessels in the PCL group remained significantly higher compared to CONTROL even after 60 days. This result can be justified, at least in part, by the maintenance of high TGF-β expression observed in the PCL group even after 60 days. Despite the more significant number of vessels observed in the HA and PCL groups, there were no statistical differences regarding vessel area between the experimental groups, probably due to the small cross-section of the capillaries. We observed increased protein expression, by immunohistochemistry and Western Blot, for fibroblast growth factor (FGF) in both HA and PCL groups compared to the CONTROL group. Fibroblast growth factors (FGFs) are broad-spectrum mitogens and regulate cellular functions, including migration, proliferation, differentiation, and survival. FGF signaling is essential in tissue development, metabolism, and homeostasis [38]. FGF family members increase fibroblast proliferation and activation, stimulating collagen accumulation and angiogenesis, and are essential in tissue repair [39–41].

Our data reinforce these studies since the higher protein expression of FGF was accompanied by a significant increase in fibroblasts, blood vessels, and collagen in tissue inoculated by both fillers evaluated. Collagen deposition was assessed in the connective tissue adjacent to the HA and PCL mass by Picrosirius Red staining under polarized light. There was a more significant deposition of collagen III, at 30 days, in PCL compared to HA, probably related to the increase of FGF already in this period. In 60 days, there was a significant reduction of collagen III in groups HA and PCL compared to the previous period, with no significant difference between HA and PCL. When type I collagen was evaluated, there were no differences between HA and PCL in the periods considered. It is known that collagen is the dominant component of the ECM in the dermis and accounts for approximately 70% of its dry weight.

Furthermore, in intact adult skin, the ratio of collagen I to collagen III is approximately 4: 1. The amount of collagen III increases temporarily when the skin is injured and during neoderm formation. In freshly healed human skin, the ratio of collagen I to collagen III is about 1: 1, as in neonatal skin. At the same time, in response to a wound, the skin may have a higher amount of collagen III and hyaluronic acid and a lower amount of collagen I [42]. The higher amount of collagen III observed in our analyses is probably associated with the natural tissue repair and healing process, which initially forms collagen III.

In 2014, Kim and colleagues investigated whether PCL-based dermal filler induced neocollagenesis in human tissue in a pilot study by histological analysis. Two patients indicated for temple lift surgery were included in the study. PCL was injected intradermally into the temporal region, just below the hairline, which would be included in lift surgery, 13 months after injection. Tissue collected after surgery showed collagen formation around the PCL particles, maintained even 13 months after injection [31].

Another study compared neocollagenesis and elastin production stimulated by Radiesse® (calcium hydroxylapatite; CHAA, Merz Pharmaceuticals GmbH) and Juvéderm® VOLUMA®, the same HA used in the present study. Twenty-four women received subperiosteal injections in the retroauricular region, and punch biopsies were performed 4 and 9 months after the injections. The authors noted that type I collagen gradually replaced type III collagen after 9 months of injection [43]. An animal study using Ellansé showed the formation of type III and type I collagen after nine months of biomaterial injection. After 21 months, the predominance of type I collagen deposited around the PCL microspheres suggests that type I collagen replaces type III collagen in the long term, such as in wound healing [20]. Based on these studies, we can deduce that with a more extended observation of the inoculated animals, we would detect a more significant amount of collagen I in our samples.

Our data reinforce literature studies showing the benefits of temporary fillers in maintaining skin volume. Although HA had a more significant volumizing effect, PCL stimulated greater collagen deposition after 30 days compared to HA. This result is reinforced by the higher number of fibroblasts observed in the PCL group. Therefore, we speculate that the greater volumization observed in the HA group is mainly due to its hygroscopic action, an already well-established effect in the literature. Ideally, in applying biocompatible materials, no exacerbated tissue reaction should be adjacent to the injected product. Mild, controlled, subclinical inflammation is expected to prolong the product's longevity. The local response of the tissue to the foreign body, through phagocytosis, is the most critical factor in determining the filler's longevity. In this process, some enzymes are present in the tissue, and free radicals break the filler into fragments that are removed by circulating macrophages and, subsequently, by lymphatic channels [44].

5. CONCLUSION

The standardized model for evaluating subcutaneous fillers proved viable, mimicking the injection plan used in humans and allowing the analysis of the cellular and morphological alterations proposed in this study. Our morphological findings demonstrate the stimulation of fibroblast activity and a related active regeneration of the connective tissue, with increased vascular proliferation and expression of markers FGF and TGF-β, related to tissue proliferation, especially in the PCL group. We observed increased adipose tissue related to the treated groups. However, no quantification was done to measure this increase, and further studies are needed to confirm this finding and investigate the role of the adipose tissue when in contact with HA and PCL. The study indicates the period evaluated induced collagen deposition, mainly type III.

Declarations

Acknowledgments: We are grateful to the Nucleus of Study in Microscopy and Image Processing (NEMPI) from the Morphology Department of Federal University of Ceará (UFC) for all histology and digital imaging services and Central Analítica-UFC (open facility funded by Finep-CT-INFRA, CAPES-Pró-Equipamentos and MCTI-CNPq-SisNano2.0).

Author contributions: Conceptualization: Leitão RFC, Góes P, Nunes APN; Funding acquisition: Brito GAC; Investigation Braga CM, Melo DBN, Rebouças CSM, Writing - original draft: Braga CM and Leitão RFC; Writing - review & editing: Leitão RFC, Braga CM Morais MLGS.

Funding: This study was partially financed by the Coordenação de Aperfeiçoamento de Pessoal de Nível Superior - Brasil (CAPES) - Finance Code 001 (PROEX 23038.000509/2020-82).

Ethical approval: This article does not contain any studies with human participants by any authors. All applicable international, national, and/or institutional guidelines for the care and use of animals were followed.

Informed consent: Not applicable to research involving animals.

Conflict of Interest: The authors declare no competing interests.

References

1. Naylor EC, Watson REB, Sherratt MJ (2011) Molecular aspects of skin aging. Maturitas 69:249–256
2. Gutowski KA (2016) Hyaluronic Acid Fillers: Science and Clinical Uses. Clin Plast Surg 43:489–496
3. Oriá RB, Valdeci F, Ferreira A, et al (2003) Study of age-related changes in human skin using histomorphometric and autofluorescence approaches. An bras Dermatol 74:425–434
4. Zerbinati N, Calligaro A (2018) Calcium hydroxylapatite treatment of human skin: Evidence of collagen turnover through picrosirius red staining and circularly polarized microscopy. Clin Cosmet Investig Dermatol 11:29–35. https://doi.org/10.2147/CCID.S143015
5. Kontis TC (2013) Contemporary review of injectable facial fillers. JAMA Facial Plast Surg 15:58–64
6. American Society for Aesthetic Plastic Surgery 2018. Available from: https://www.plasticsurgery.org/documents/News/Statistics/2018/plastic-surgery-statistics-full-report-2018.pdf
7. Schiraldi C, Gatta A La, De Rosa M (2010) Biotechnological Production and Application of Hyaluronan. Biopolymers. Sciyo. Available from: http://dx.doi.org/10.5772/10271
8. De Melo F, Nicolau P, Piovano L, et al (2017) Recommendations for volume augmentation and rejuvenation of the face and hands with the new generation polycaprolactone-based collagen stimulator (Ellansé®). Clin Cosmet Investig Dermatol 10:431–440
9. Leitão RFC, Ribeiro RA, Bellaguarda EAL, et al (2007) Role of nitric oxide on pathogenesis of 5-fluorouracil induced experimental oral mucositis in hamster. Cancer Chemother Pharmacol 59:603–

612. https://doi.org/10.1007/s00280-006-0301-y

10. Hsu S, Raine L, Fanger H (1981) The Use of Antiavidin Antibody and Avidin-Biotin-Peroxidase Complex in Immunoperoxidase Technics. Am J Clin Pathol 75: 816–21
11. Brey EM, Lalani Z, Johnston C, et al (2003) Automated Selection of DAB-labeled Tissue for Immunohistochemical Quantification. The Journal of Histochemistry & Cytochemistry 51: 575–584
12. Haneke E (2014) Adverse effects of fillers and their histopathology. Facial Plastic Surgery 30:599–614. https://doi.org/10.1055/s-0034-1396755
13. Bertossi D, Nocini PF, Rahman E, et al (2020) Non surgical facial reshaping using MD Codes. J Cosmet Dermatol 19:2219–2228. https://doi.org/10.1111/jocd.13596
14. Buck DW, Alam M, Kim JYS (2009) Injectable fillers for facial rejuvenation: a review. Journal of Plastic, Reconstructive and Aesthetic Surgery 62:11–18
15. Griffith LG (2008) Polimeric Biomaterials. Acta Materialia 48:263–277
16. HEE, C. K. et al (2015). Rheological Properties and In Vivo Performance Characteristics of Soft Tissue Fillers. Dermatologic surgery: official publication for American Society for Dermatologic Surgery 41: 373–S381
17. Cabral LRB, Teixeira LN, Gimenez RP, et al (2020) Effect of hyaluronic acid and poly-l-lactic acid dermal fillers on collagen synthesis: An in vitro and in vivo study. Clin Cosmet Investig Dermatol 13:701–710. https://doi.org/10.2147/CCID.S266015
18. Jeong SH, Fan YF, Baek JU, et al (2016) Long-lasting and bioactive hyaluronic acid-hydroxyapatite composite hydrogels for injectable dermal fillers: Physical properties and in vivo durability. J Biomater Appl 31:464–474. https://doi.org/10.1177/0885328216648809
19. Lee SJ, Lee WS, Chung CH (2019) Safety and efficacy of polycaprolactone copolymer nanosphere hydrogel injected into the scalp dermal tissue of rats. Archives of Aesthetic Plastic Surgery 25:147–153. https://doi.org/10.14730/aaps.2019.01739
20. Nicolau pierre J, Marijnissen-Hofsté J, Nicolau PJ (2013) original Article The European Journal of Aesthetic Medicine and Dermatology. Medicine and Dermatology 3:19–26
21. Nadra K, André M, Marchaud E, et al (2021) A hyaluronic acid-based filler reduces lipolysis in human mature adipocytes and maintains adherence and lipid accumulation of long-term differentiated human preadipocytes. J Cosmet Dermatol 20:1474–1482. https://doi.org/10.1111/jocd.13794
22. Rippa AL, Kalabusheva EP, Vorotelyak EA (2019) Regeneration of dermis: Scarring and cells involved. Cells 8:607 https://doi.org/10.3390/cells8060607
23. Driskell RR, Jahoda CAB, Chuong CM, et al (2014) Defining dermal adipose tissue. Exp Dermatol 23:629–631
24. Kim JA, Van Abel D (2015) Neocollagenesis in human tissue injected with a polycaprolactone-based dermal filler. Journal of Cosmetic and Laser Therapy 17:99–101. https://doi.org/10.3109/14764172.2014.968586

25. Stocks D, Sundaram H, Michaels J, et al (2011). Rheological evaluation of the physical properties of hyaluronic acid dermal fillers. Journal of Drugs in Dermatology: 10: 974–980. PMID: 22052265.
26. Signorini M, Liew S, Sundaram H, et al (2016) Global Aesthetics Consensus: Avoidance and Management of Complications from Hyaluronic Acid Fillers - Evidence- and Opinion-Based Review and Consensus Recommendations. Plast Reconstr Surg 137:961e–971e
27. Brandt FS, Cazzaniga A (2008) Hyaluronic acid gel fillers in the management of facial aging Clin Interv Aging 3:153–9
28. Farahani SS, Sexton J, Stone JD, et al (2012) Lip Nodules Caused by Hyaluronic Acid Filler Injection: Report of Three Cases. Head Neck Pathol 6:16–20. https://doi.org/10.1007/s12105-011-0304-9
29. Christensen LH, Nielsen JB, Mouritsen L, et al (2008) Tissue integration of polyacrylamide hydrogel: An experimental study of periurethral, perivesical, and mammary gland tissue in the pig. Dermatologic Surgery 34:S68-77 https://doi.org/10.1111/j.1524-4725.2008.34246.x
30. Guo J, Guo S, Wang Y, Yu Y (2017) Adipose-derived stem cells and hyaluronic acid based gel compatibility, studied in vitro. Mol Med Rep 16:4095–4100. https://doi.org/10.3892/mmr.2017.7055
31. Kim JA, Van Abel D (2015) Neocollagenesis in human tissue injected with a polycaprolactone-based dermal filler. Journal of Cosmetic and Laser Therapy 17:99–101. https://doi.org/10.3109/14764172.2014.968586
32. Zdolsek J, Eaton JW, Tang L (2007) Histamine release and fibrinogen adsorption mediate acute inflammatory responses to biomaterial implants in humans. J Transl Med 5: 31 https://doi.org/10.1186/1479-5876-5-31
33. Gilbert RWD, Vickaryous MK, Viloria-Petit AM (2016) Signalling by transforming growth factor beta isoforms in wound healing and tissue regeneration. J Dev Biol 4:21
34. Varga J, Rosenbloomt J, Jimenez SA (1987) Transforming growth factor (TGFf) causes a persistent increase in steady-state amounts of type I and type III collagen and fibronectin mRNAs in normal human dermal fibroblasts. Biochem J 247:597–604
35. Nevers T, Salvador AM, Velazquez F, et al (2017) Th1 effector T cells selectively orchestrate cardiac fibrosis in nonischemic heart failure. Journal of Experimental Medicine 214:3311–3329. https://doi.org/10.1084/jem.20161791
36. Darby IA, Hewitson TD (2007) Fibroblast Differentiation in Wound Healing and Fibrosis. Int Rev Cytol 257:143–179
37. Frangogiannis NG (2020) Transforming growth factor–ß in tissue fibrosis. Journal of Experimental Medicine 217:e20190103.
38. Xie Y, Su N, Yang J, et al (2020) FGF/FGFR signaling in health and disease. Signal Transduct Target Ther 5:181
39. De Araújo R, Lôbo M, Trindade K, et al (2019) Fibroblast Growth Factors: A Controlling Mechanism of Skin Aging. Skin Pharmacol Physiol 32:275–282

40. Murakami M, Simons M (2008) Fibroblast growth factor regulation of neovascularization. Curr Opin Hematol 15:215–220
41. Turner N, Grose R (2010) Fibroblast growth factor signalling: From development to cancer. Nat Rev Cancer 10:116–129
42. Woodley DT (2017) Distinct Fibroblasts in the Papillary and Reticular Dermis: Implications for Wound Healing. Dermatol Clin 35:95–100
43. Yutskovskaya Y.; Kogan E.; Leshunov E (2014). A randomized, split-face, histomorphologic study comparing a volumetric calcium hydroxylapatite and a hyaluronic acid-based dermal filler. J Drugs Dermatol 13: 1047–1052, 2014.
44. Bentkover SH (2009) The biology of facial fillers. Facial Plastic Surgery 25:73–85

Figures

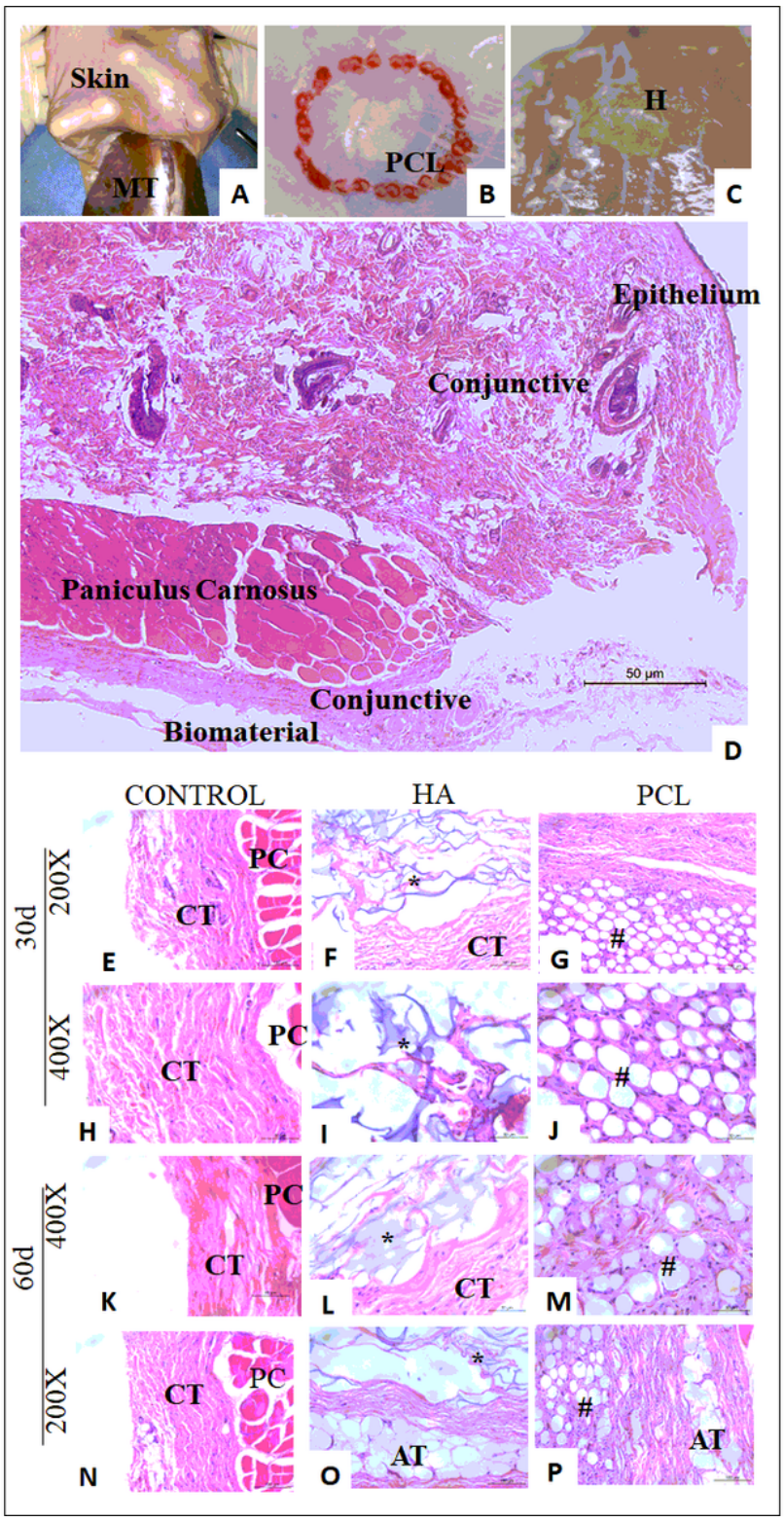

Figure 1

Macroscopy and microscopy of rat skin after injection of PCL (#) and HA (*). **A**, The animal's skin reveals muscle tissue (MT) **B**, Visual inspection of PCL. **C**, Visual inspection of HA. **D**, Microscopic topography of the mouse skin highlights panniculus carnosus (40x magnification). **E**, **H**, **K**are photomicrographs of untreated skin at 30 and 60 days (CONTROL group). **F**,**I**, and **L** are photomicrographs of HA-treated skin.

G, **J**, and **M** are photomicrographs of PCL-treated skin. **N**, **O**, and **P**show the presence of adipose tissue (AT) in the loose connective tissue (CT), below the panniculus carnosus, in the HA and PCL groups.

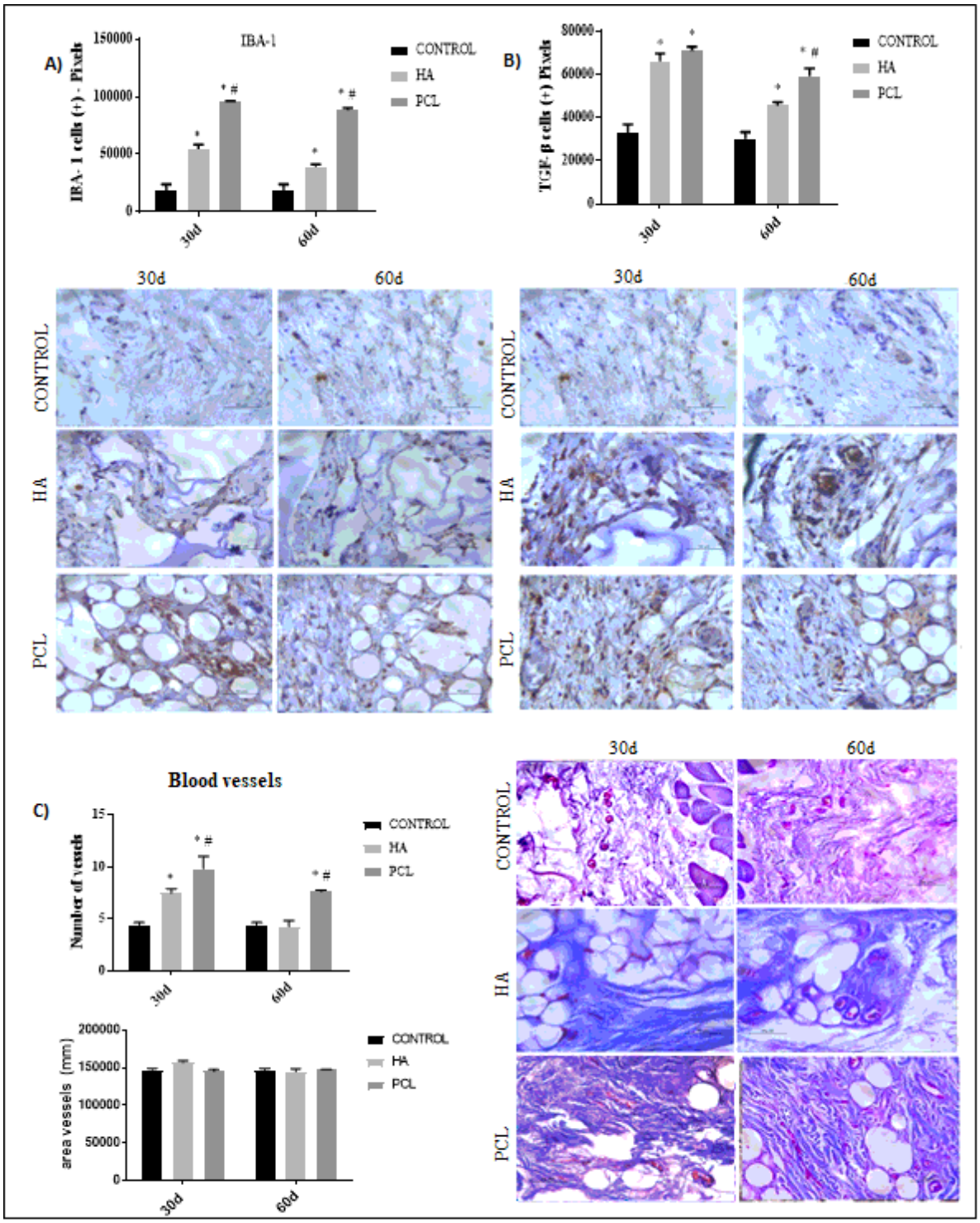

Figure 2

Immunohistochemistry for IBA-1, TGF-β, and analysis of neovascularization using Mallory's Trichrome. **A**. Immunostaining for IBA-1 at 30 and 60 days and quantifying activated macrophages. **B**. immunostaining

for TGF-β at 30 and 60 days and quantification expressed in the graph. **C**. Measurement of the area of the vessels on the periphery of the biomaterials and quantification of vessels after 30 and 60 days. Bars show mean ± SEM of 6 animals per group. * Represents the significant difference in HA and PCL compared to CONTROL at 30 and 60 days. # Represents the significant difference between PCL and HA. (*p< 0.001), ANOVA followed by Tukey's test).

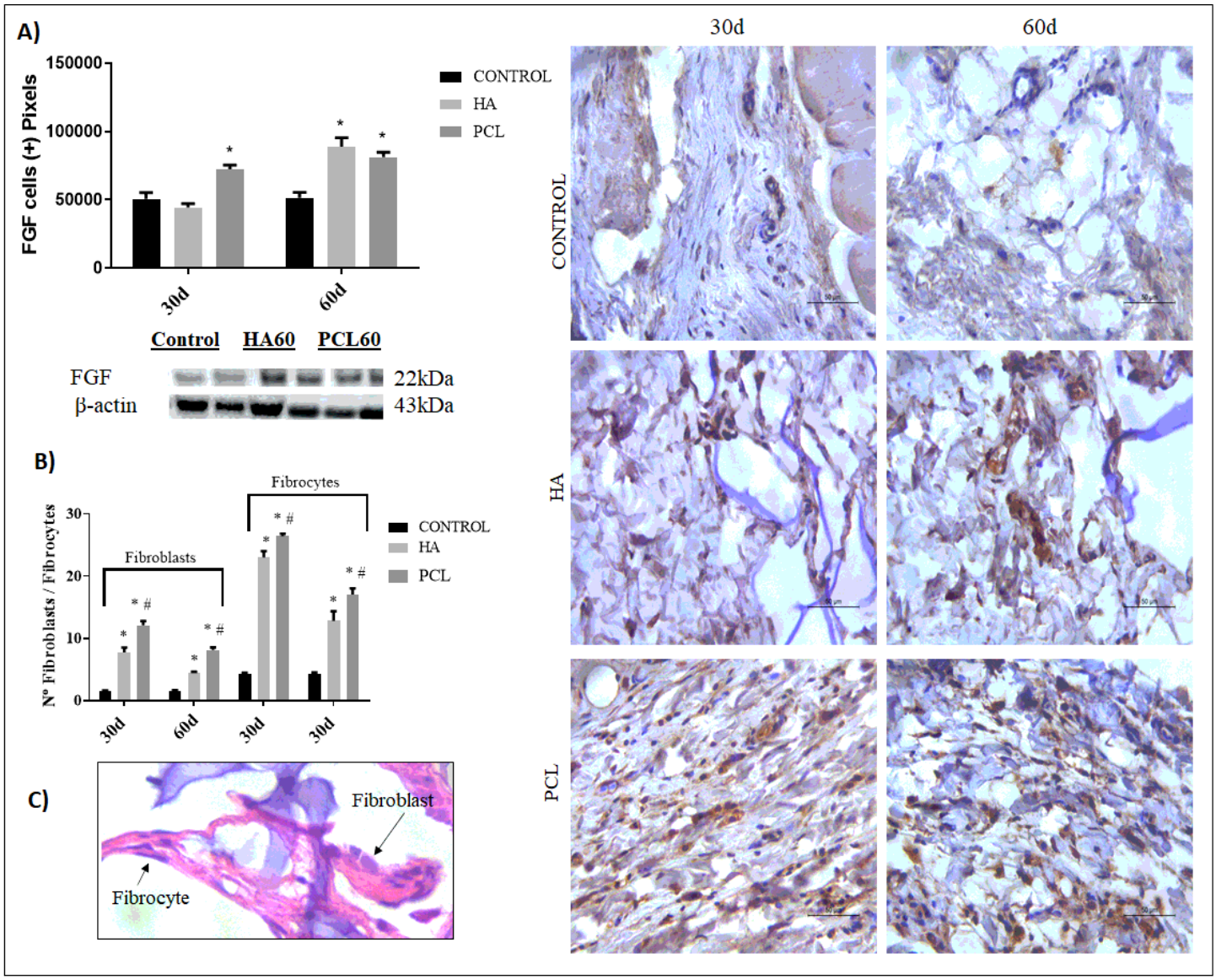

Figure 3

Number of fibroblasts / fibrocytes, immunostaining and FGF protein expression.

A. Immunostaining for FGF at 30 and 60 days and quantification of 1 expressed in the graph. **B.**Fibrocyte and fibroblast count at 30 and 60 days represented in the graph. **C.**Illustrative image of the fibrocyte and fibroblast in the connective tissue adjacent to the biomaterial. Bars show mean ± SEM of 6 animals per group. * represents the significant difference of HA and PCL when compared to CONTROL, at 30 and 60

days. # represents the significant difference between PCL and HA. (*p< 0.001), ANOVA followed by Tukey's test).

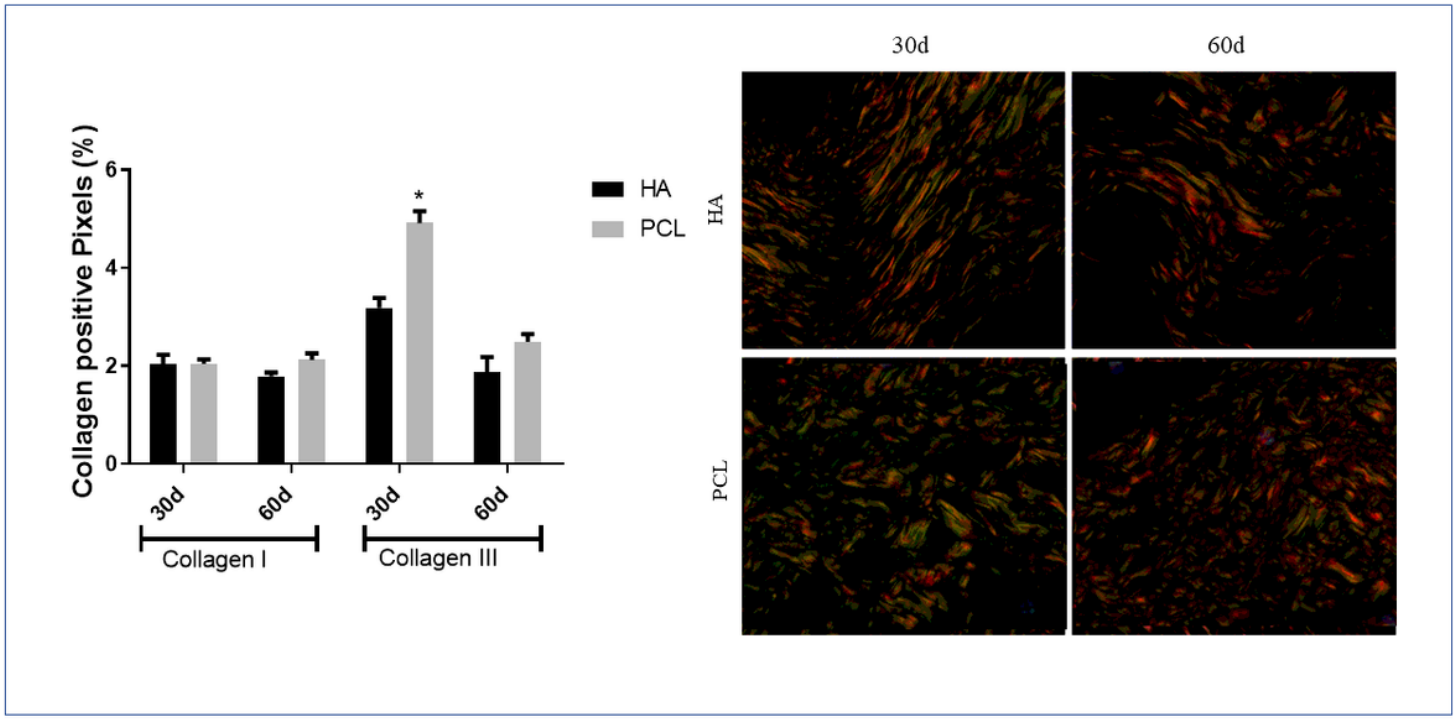

Figure 4

Graph representing the quantification of type I and III collagen fibers stained with Picrosirius Red and photomicrography of the skin of rats in the HA and PCL experimental groups. * Represents a significant difference in PCL compared to HA at 30 days. (*p< 0.001), ANOVA followed by Tukey's test. It is possible to observe the presence of collagen type I (red) and III (green). 400x magnification.